Nanoscale

PAPER

View Article Online
View Journal | View Issue

Cite this: *Nanoscale*, 2017, **9**, 1862

The supercoiling state of DNA determines the handedness of both H3 and CENP-A nucleosomes†

R. Vlijm,‡[a] S. H. Kim,[a] P. L. De Zwart,[a] Y. Dalal*[b] and C. Dekker*[a]

Received 6th August 2016,
Accepted 8th January 2017

DOI: 10.1039/c6nr06245h

rsc.li/nanoscale

Nucleosomes form the unit structure of the genome in eukaryotes, thereby constituting a fundamental tenet of chromatin biology. In canonical nucleosomes, DNA wraps around the histone octamer in a left-handed toroidal ramp. Here, in single-molecule magnetic tweezers studies of chaperone-assisted nucleosome assembly, we show that the handedness of the DNA wrapping around the nucleosome core is intrinsically ambidextrous, and depends on the pre-assembly supercoiling state of the DNA, *i.e.*, it is not uniquely determined by the octameric histone core. Nucleosomes assembled onto negatively supercoiled DNA are found to exhibit a left-handed conformation, whereas assembly onto positively supercoiled DNA results in right-handed nucleosomes. This intrinsic flexibility to adopt both chiralities is observed both for canonical H3 nucleosomes, and for centromere-specific variant CENP-A nucleosomes. These data support recent advances suggesting an intrinsic adaptability of the nucleosome, and provide insights into how nucleosomes might rapidly re-assemble after cellular processes that generate positive supercoiling *in vivo*.

Introduction

In eukaryotic cells, DNA wraps around histone octamers to form nucleosomes. These particles compact the genome, and mediate accessibility to the underlying DNA, thus regulating major cellular processes like transcription, replication and repair. Hence, the structure of nucleosomes has been the focus of many studies.[1–6] As the vast majority of nucleosome structural studies show, DNA wraps around the core histones in a left-handed ramp, with the histones inserting Arginines into the minor groove of DNA once every ~10.4 bp. Thus, 147 bp of DNA are arranged in 14 segments of a left-handed super-helical ramp around the octamer. Under specialized circumstances, there has been evidence for a minor fraction of nucleosomes existing in right-handed, partial, pre-nucleosomal, and unfolded forms.[8–10] Furthermore, similar to tetrameric nucleosomes found in the archaebacteria,[11–13] which can flip between right and left handed states, H3/H4 tetrasomes can adopt a left- or right-handed chirality. Flexibility in the manner in which DNA wraps about the core particle may thus arise from intrinsic adaptability of the H3/H4 interface. Indeed, recent work[18–20] supports early pioneering papers[21–23] showing that H3/H4 tetrasomes can inter-convert between the right- and left-handed states. While early work in the chromatin field demonstrated that octameric nucleosomes are preferentially assembled onto negatively supercoiled DNA,[24,25] absorbing the negative DNA plectonemes into the left-handed wrap found in the canonical octamer, more recent work has argued for the presence of "reversomes", transitionary forms used by nucleosomes to switch between handedness.[8,26] Adding to this topological complexity, histone variants such as CENP-A, which replace H3 in centromere-specific nucleosomes, have been correlated with positive supercoils on closed circular mini-plasmids *in vivo* in yeast, and *in vitro*.[9,10] In contrast, the human version of CENP-A nucleosomes has been reported to constrain only a traditional left-handed wrap *in vitro*.[2] Surprisingly, despite potential differences in supercoiling state, yeast CENP-A can functionally rescue human CENP-A depletion in human cells, suggesting an embedded memory of the correct nucleosomal shape needed for mitotic function.[27] Finally, the surprising discovery of large tracts of positively supercoiled domains within human cells[28,29] leads to two key biological questions that remain unaddressed: namely, whether histone chaperones can assemble histones on positively supercoiled DNA templates; and, what handedness such nucleosomes might possess.

To obtain insights into these fundamental questions, we used single-molecule magnetic tweezers to examine whether

[a]*Department of Bionanoscience, Kavli Institute of Nanoscience Delft, Delft University of Technology, Delft, 2628CJ, The Netherlands*
[b]*Chromatin Structure and Epigenetic Mechanisms Unit, Laboratory of Receptor Biology and Gene Expression, Center for Cancer Research, National Cancer Institute, NIH, Bethesda, MD, 20892, USA. E-mail: dalaly@mail.nih.gov, C.Dekker@tudelft.nl*
†Electronic supplementary information (ESI) available. See DOI: 10.1039/c6nr06245h
‡Current address: Division of Optical Nanoscopy, German Cancer Research Center, Heidelberg, Germany.

canonical and variant nucleosomes can be assembled on DNA with varying levels of supercoiling, including positively twisted DNA. Magnetic tweezers are exquisitely suited to address this question, because this tool permits the application of well-defined supercoiling densities to individual DNA molecules prior to assembly. As has been well established in the literature,[8,14,18,30] it also allows for an unambiguous determination of the linking number of nucleosomes assembled onto each single DNA molecule. Opposed to experiments on circular DNA, we have rotational control over a linear DNA fragment. Therefore, we can relax the linker DNA after nucleosome assembly to remove potential cross-over of the entry and exit DNA. The measured linking number in our assay is thus purely a result from the assembled nucleosomes. Here, we report that both H3 and CENP-A nucleosomes can assemble efficiently on both negatively and positively supercoiled DNA. Consistent with decades of biochemical work, applying negative supercoiling of the DNA before assembly in this assay led to the formation of primarily left-handed nucleosomes. In contrast, positive supercoiling of the DNA ahead of assembly also led to the efficient formation of nucleosomes, but, surprisingly, these nucleosomes possessed a right-handed chirality. These data suggest that positive supercoiling is not, *a priori*, inhibitory to nucleosome assembly, but rather support a model in which canonical and histone-variant nucleosomes can tolerate a right-handed chirality, and could potentially occupy positively supercoiled DNA *in vivo*. More generally, the data also demonstrate that the handedness of the DNA wrapping around the nucleosome core depends not on any specific histone variant, but rather on the pre-assembly supercoiling state of the DNA upon which it is assembled.

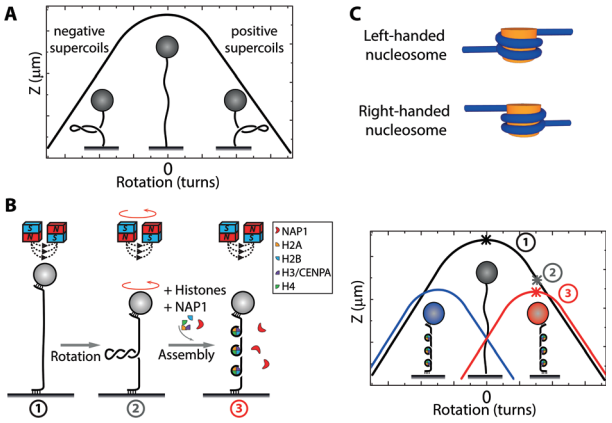

Fig. 1 Single-molecule magnetic tweezers. (A) Rotation curve of a supercoiled DNA molecule. The black line represents a typical rotation curve of a rotationally constrained dsDNA molecule. At constant force (≤0.6 pN), the maximal DNA end-to-end length *Z* occurs in the absence of externally applied rotations. When negative/positive turns are applied, initially the induced linking number is absorbed by under/overwinding of the DNA backbone (twist). After a certain buckling point, extra turns are absorbed by the formation of plectonemic supercoils (writhe) which reduces *Z*. The cartoons illustrate how negative and positive supercoils decrease the DNA end-to-end length compared to relaxed DNA. (B) Schematic overview of a magnetic tweezers experiment. (1) In a flow cell, a double stranded DNA (dsDNA) molecule with multiple DIG-labels at one end is tethered to an anti-DIG coated glass surface. The other end of the DNA molecule contains multiple biotin labels, which bind to the streptavidin-coated super-paramagnetic bead. A pair of magnets is placed above the flow cell, inducing a vertical pulling force, which stretches the DNA molecule. To make a rotation curve, the pair of magnets is rotated, which rotates the superparamagnetic beads. As the DNA molecule is rotationally constrained, the linking number of the DNA is changed by the number of applied magnet rotations. In the applied force regime of 0.3 pN, rotating the magnets induces plectonemic supercoil formation. Over a range of approximately −20 turns to +20 turns, the DNA end-to-end length *Z* is measured as a function of the applied rotations, resulting in a rotation curve as shown in black in the right panel. The black asterisk indicates the position at which the bare DNA is torsionally relaxed. (2) Consecutively, a specific number of positive or negative rotations is applied, which decreases *Z* due to supercoil formation (grey cross in right panel for the example of positive supercoiling). (3) After inducing the desired amount of supercoiling to the DNA, histones (colored quarter circles) and the histone chaperone NAP1 (red crescents) are flushed into the flow cell to form nucleosomes. The new rotation curve is similar to the red (when positive supercoiling was applied) or blue curve (when negative supercoiling was applied). The positive (negative) shift of the red (blue) rotation curve indicates that the formed nucleosomes are right- (left-) handed. A more detailed overview of the measurement setup is shown in Fig. S1.† (C) Depiction of the wrapping of DNA around the histone octamer in a left- or right-handed nucleosome.

Material & methods

Magnetic tweezers

Magnetic tweezers have the unique advantage of exerting a precisely defined degree of supercoiling to a single DNA molecule *prior* to nucleosome assembly, without the need for low-yield enzymatic treatment (*e.g.* gyrase[31]), or intercalating chemicals.[32,33] Intercalating chemicals such as ethidium bromide or chloroquine vastly increase the likelihood of UV-induced nicks, resulting in the immediate loss of supercoiling, making experimental investigations using this tool tedious. Indeed, prior experiments on pre-supercoiled DNA (other than magnetic tweezers) have been highly technically challenging for precisely this reason. Because DNA exists *in vivo* in both negatively and positively supercoiled states in eukaryotes,[28] it is relevant to examine how chromatin assembly is impacted by the intrinsic supercoiling state of DNA. Magnetic tweezers offer an attractive experimental tool to investigate an otherwise intractable biological problem.

In a magnetic tweezers experimental setup (Fig. 1), a double stranded DNA (dsDNA) molecule is tethered between a glass surface and a super-paramagnetic bead in a flow cell, resulting in a rotationally constrained molecule (see Fig. S1A† for detailed experimental setup). In our magnetic tweezers, the end-to-end length of a single DNA molecule is measured in real time[34] at 100 Hz with a precision of a few nanometers. The applied stretching force and supercoiling density can be set by the height and applied rotations of a pair of magnets held above the bead. Each single DNA molecule is characterized prior to nucleosome assembly by measuring the rotation curve at very low (0.3 pN) stretching force (Fig. 1A). Consecutively, positive or negative

supercoiling is applied by rotating the magnets (Fig. 1B). Using this method, we applied between −20 and +20 coils to a 7.9 kb long dsDNA construct (*i.e.* a supercoiling density σ between −2.6% and +2.6%). Next, recombinant histones H3 (or CENP-A), H4, H2A and H2B and histone chaperone NAP1 are flushed in (see Nucleosome assembly and buffer conditions). During the flush, a stretching force above 3 pN was applied to the tethered DNA molecule to hinder nucleosome assembly, and to prevent sticking of the magnetic bead to the glass surface. Immediately after the protein flush is finished, the force was lowered again to 1 pN to permit chaperone-mediated nucleosome assembly (Fig. 1B). For these measurements, it is important to note that we adjusted the protein concentration such that DNA molecules were sub-saturated with nucleosomes (with only 1–24 nucleosomes assembled onto the 7.9 kb dsDNA), thus maintaining enough linker DNA to measure an accurate rotation curve. Thus, in order to study the handedness of individual nucleosomes, we intentionally kept the number of assembled nucleosomes low.

Magnetic tweezers provide precise control of the supercoiling in the DNA molecule of interest, with a set linking number L_k. The linking number of a DNA molecule is the sum of the twist (Tw) within the DNA duplex and the writhe (Wr) due to the supercoiling of DNA around itself in plectonemic loops. In a rotationally constrained molecule, the induced magnet rotations ΔL_k can be absorbed in a change in helical twist of the dsDNA backbones (Tw) and/or in a change in the number of plectonemes (Wr), *i.e.*, $\Delta L_k = \Delta Tw + \Delta Wr$. Nucleosome formation can change the linking number and we extract the linking number of the assembled nucleosomes, $\Delta L_{k,nuc}$, by comparing the linking number of the DNA molecule containing the nucleosomes with that of the bare DNA before the assembly. We do so by measuring rotation curves where we monitor, at a constant force of 0.3 pN, the end-to-end length Z of a single dsDNA molecule as a function of applied supercoiling density. The cartoons in Fig. 1A illustrate how both negative and positive supercoils decrease Z compared to relaxed DNA. After the assembly of nucleosomes, a new rotation curve is measured (Fig. 1B) and two differences are observed: first, the maximum of the curve is lower, as the nucleosomes have compacted the DNA molecule. Second, the center of the rotation curve has shifted by a certain number of turns upon nucleosome assembly, due to the nucleosome-wrapping-associated change in the linking number. The shift in the center of the rotation curve is therefore a direct measure of the total linking number of the assembled nucleosomes, $\Delta L_{k,nuc}$. In total 56 individual DNA molecules were measured in detail to establish the findings reported here.

Protein expression and purification

Recombinant CENP-A, H3, H4, H2A and H2B histones were purified according to the protocol from Luger and colleagues,[35] with modifications detailed in Walkiewicz *et al.*[36] Purified recombinant NAP-1 and the core histones used for Fig. S5† were a kind gift by Alexandra Lusser and purified as described in Vlijm *et al.*[18]

Nucleosome assembly and buffer conditions

In all experiments, the measurement buffer consisted of 50 mM KCl, 25 mM Hepes-KOH pH 7.6, 0.1 mM Ethylenediaminetetraacetic acid (EDTA), 0.038% Polyethylene Glycol (PEG), 0.038% Polyvinyl Alcohol (PVOH), adapted from ref. 14. PEG and PVOH were added as crowding agents. For nucleosome assembly, we used recombinant mammalian histones H2A, H2B, H4 and either H3 or CENP-A, together with the histone chaperone NAP1, which assembles complete nucleosomes *in vitro*.[14,37–41] Before each experiment, histones and NAP1 were pre-incubated on ice for 30 minutes and, unless stated differently, at the following concentrations: for canonical nucleosomes: 184 nM H3, 184 nM H4, 484 nM H2A, 484 nM H2B, and 621 nM NAP1; for CENP-A nucleosomes, 105 nM CENP-A, 105 nM H4, 655 nM H2A, 655 nM H2B, and 274 nM NAP1. A higher concentration of H2A/H2B dimers with respect to the other core histones was used to promote full nucleosome formation over potential (CENP-A/H4 or H3/H4) tetrasome formation. The pre-incubation buffer contained 50 mM KCl, 25 mM Hepes pH 7.6, 0.1 mM EDTA, 0.25% PEG, 0.25% PVOH and 1 mg ml^{-1} BSA. Just prior to flushing in, the protein concentration was reduced ~2000 fold by dilution with the measurement buffer, to establish conditions where only a limited number of nucleosomes was assembled onto the DNA in the magnetic tweezers.

DNA constructs

We used a 7.9 kilo-base-pair (kbp) double-stranded DNA (dsDNA) molecule lacking any nucleosome-positioning sequences that potentially can induce anomalous nucleosome structures. The DNA construct was a fragment obtained from the pBlueScript-1,2,4+pSfv1 plasmid, which was made by introducing fragments of Lambda DNA and a fragment from pSfv1 (Invitrogen) in pBluescript SK+ (Agilent). The final construct contained mostly Lambda DNA, but also part of the pSfv1 vector. The GC content along the molecule is shown in Fig. S1B,† with a moving average of 150 bp, and the complete sequence is given in the ESI.† To tether the DNA, the ends of the molecules were labeled with multiple digoxigenin molecules at one end and multiple biotin molecules at the other end. We used 2.8 μm diameter streptavidin-coated superparamagnetic beads (Dynabeads® M-270 Streptavidin) to connect a magnetic bead at the biotin labeled end of the DNA molecule.

Results

Left-handed nucleosomes form on negatively supercoiled DNA, whereas right-handed nucleosomes form on positively supercoiled DNA

We first examined the effect of negative supercoiling on nucleosome assembly. We generated negative supercoiling by applying up to 17 negative turns (−2.2% supercoiling density) to the DNA molecules before assembling canonical (H2A, H2B, H3 and H4) or centromeric (H2A, H2B, CENP-A, H4) nucleosomes in the presence of the histone chaperone NAP1 (see

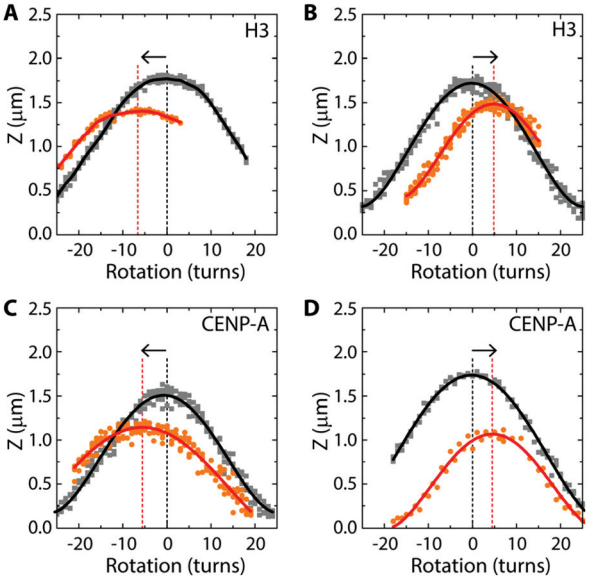

Fig. 2 Representative rotation curves before and after nucleosomes are assembled on supercoiled DNA. Typical rotation curves measured before (gray squares) and after (orange circles) nucleosome assembly, at an applied force of 0.3 pN. Thick solid lines are guides to eye (4th order polynomial fit). Dotted lines indicate the center of each rotation curve (black is before, and red is after nucleosome assembly). The applied rotations before the assembly are −5 (A), +5 (B), −10 (C) and +7 (D) turns. (A) H3 nucleosomes are found to be left-handed when assembled onto negatively supercoiled DNA, as the rotation curve is shifted by 7 ± 2 turns to the left. (B) H3 nucleosomes are found to be right-handed on positive supercoiled DNA, as the rotation curve is shifted by 5 ± 1 turns to the right. (C) CENP-A nucleosomes are, similar to H3 nucleosomes, found to be left-handed when formed onto negatively supercoiled DNA, as the rotation curve shifts by 6 ± 1 turns to the left. (D) CENP-A nucleosomes are found to be right-handed when assembled onto positively supercoiled DNA, as the rotation curve shifts 4 ± 1 turns to the right. More examples are shown in the Fig. S2.†

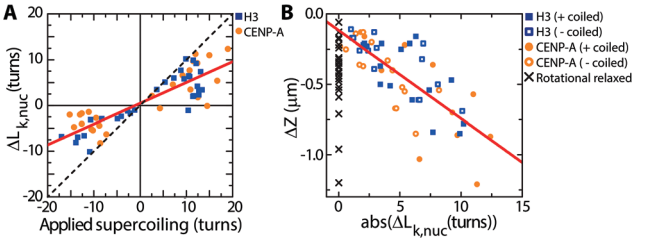

Fig. 3 Linking number change and compaction upon nucleosome assembly. (A) Dependence of the linking number change on the applied supercoiling. The shift of the center of the rotation curve measures the change in linking number ($L_{k,nuc}$) due to nucleosome assembly. In panel A, the total linking number of the assembled nucleosomes ($\Delta L_{k,nuc}$) is plotted as a function of the amount of supercoiling that is applied to the DNA before assembly of nucleosomes. Both H3 (blue squares) and CENP-A (orange circles) nucleosomes show similar results: when negative supercoiling is applied, left-handed nucleosomes are formed, whereas positive applied supercoiling leads to right-handed nucleosomes. The solid red line is the average of the linear fits of both H3 and CENP-A nucleosomes with a slope of 0.45 ± 0.04, which is very similar to the slopes of H3 (0.49 ± 0.05) and CENP-A (0.43 ± 0.06) individually. The black dotted line denotes slope 1. (B) Change ΔZ in DNA end-to-end length due to the assembly of nucleosomes, as a function of the total linking number of the nucleosomes (which is deduced from the horizontal shift of the rotation curve arising from nucleosome assembly). Both data for H3 (blue squares) and CENP-A (orange circles) are shown. The absolute value of the linking number is shown, such that results based on positive (filled) and negative supercoiled DNA (empty) can be compared. The red solid line is a linear fit to all data (slope = −63 ± 7 nm per turn). The slopes for H3 on positively and negatively coiled DNA (−63 ± 16 and −48 ± 11 nm per turn, respectively) and for CENP-A on positively and negatively coiled DNA (−69 ± 51 and −68 ± 16 nm per turn, respectively) are not significantly different. For comparison, the total amount of compaction after H3 nucleosome assembly on rotationally unconstrained (*i.e.*, nicked) molecules is shown as well (black crosses).

Material & methods for details on histone and NAP1 concentrations). The rotation curves taken after assembly were consistently shifted to the left, as indicated in the typical example in Fig. 2A (see Fig. S2† for more examples). These data show that the assembled nucleosomes have a negative linking number $\Delta L_{k,nuc}$ (to be quantified below, Fig. 3), and are thus left-handed (for a cartoon of such a nucleosome see Fig. 1C). This result is in agreement with 30 years of biochemical experiments in the chromatin field.[1,42–47] The results from identical experiments performed with the centromere histone CENP-A, exemplified in Fig. 2C, similarly showed a consistent shift to the left of the rotation curve. For CENP-A on a negatively supercoiled substrate, we thus also measured $\Delta L_{k,nuc} < 0$, and conclude that left-handed CENP-A nucleosomes were formed. These data are entirely consistent with the recently described crystal structure of the CENP-A octameric nucleosome, in which a left-handed superhelical path of DNA around the octamer was observed.[2]

Next, we examined the consequence of starting with a positively supercoiled DNA template, generated by applying up to +19 turns (supercoiling density +2.5%) to the tethered template DNA (Fig. 1). Remarkably, upon nucleosome assembly for canonical nucleosomes containing H3 in the presence of positive supercoiling, the rotation curves of DNA with nucleosomes shifted to the right (Fig. 2B, the orange nucleosome rotation curve is shifted to the right compared to the grey bare DNA curve). Because the shift of the rotation curve is a direct measure of the change in linking number,[48] $\Delta L_{k,nuc}$ can be concluded to be positive. Thus, H3 nucleosomes have assembled in a right-handed fashion on the positively supercoiled DNA (for a cartoon of such a nucleosome, see Fig. 1C). This finding is consistent with early findings that H3 nucleosomes can assemble on positively supercoiled DNA *in vitro*,[24,49] and indicates that these H3 nucleosomes can adopt a positive wrapping of the DNA around the octamer. We similarly tested assembly of CENP-A nucleosomes on the same positively supercoiled DNA templates. The data show that CENP-A containing nucleosomes also assembled efficiently on positively supercoiled DNA, exhibiting a positive ΔL_k (Fig. 2D), indicating a right-handed superhelical wrap of the DNA around the histone core.

These findings were verified by repeating these experiments for many molecules with different amounts of applied supercoiling (56 individual experiments). As Fig. 3A shows, we

observe that, in general, the total linking number of the assembled nucleosomes was greater for larger supercoiling densities applied, and this was equally true for both negative and positive supercoiling. A linear fit to the data indicates a total nucleosome linking number of +0.45 per applied supercoil. The handedness of H3- and CENP-A-containing nucleosomes was very similar under the same applied supercoiling densities (Fig. 3A). The significant spread in the linking number of the chromatinized DNA can be explained by the (intentional) sub-saturated density of assembled nucleosomes on the template DNA: assembling less nucleosomes than necessary to absorb all applied supercoiling, should give a relatively small $\Delta L_{k,nuc}$ compared to the applied number of turns – which indeed is what we observe in Fig. 3 (and further illustrated in detail in Fig. S3A and B†). Interestingly, we observe that $\Delta L_{k,nuc}$, the change in linking number due to nucleosome assembly, is never larger than the number of applied supercoils. This can be understood as follows: in the presence of positive (or negative) supercoiling, right- (or left-) handed nucleosomes are being formed, which decreases the number of DNA plectonemes. When the supercoiling is entirely reduced by the formation of nucleosomes, the intermediate linker DNA thus has a supercoil density near zero, and there is no longer a drive to assemble nucleosomes of a preferred handedness (see Fig. S3C and D†). In our previous studies of nucleosome assembly in the absence of supercoiling,[18,19] nucleosomes were all assembled in a left-handed wrapping. Based on that result, one might expect some bias in the data of Fig. 3A toward left-handed nucleosomes. As we did not observe this, the energy difference between the left- and right-handed nucleosome confirmations is likely low.

We verified that complete nucleosomes are assembled with both bulk and single-molecule control experiments. Briefly, using the classical MNase protection assay,[50,51] after assembly of the nucleosomes, the chromatin was gently digested with micrococcal nuclease. Subsequently, the digested chromatin was de-proteinized and the resulting DNA was examined by gel electrophoresis. Nuclease-protected mononucleosomal bands (120–150 bp) in the chromatinized samples *vs.* controls confirmed the successful assembly of full octameric nucleosome for both CENP-A and H3 nucleosomes.[41] To exclude effects induced by the binding of the histone chaperone NAP1, a number of single-molecule control experiments were performed (Fig. S4†). First, we studied the effect of the presence of NAP1, the histone chaperone that was employed to ensure correct binding of the histones and to prevent non-specific histone binding. After flushing in a buffer containing only the chaperone NAP1 (Fig. S4A†), the rotation curve remained undistinguishable from the rotation curve of bare DNA. In agreement with previous reports,[14,18] the presence of NAP1 in the flow cell thus did not change any of the measurable characteristics of the DNA such as its end-to-end extension Z, linking number L_k, or the persistence length[52,53] which could change upon protein binding.[54–58]

Second, we performed assembly experiments with NAP1 and H2A/H2B only, in the absence of H3/CENP-A and H4 (Fig. S4B†). Again we found that the rotations curves in the absence and presence of the proteins are identical, indicating that there is no significant non-specific binding of histones which potentially could cause aggregation and thus a decrease of the DNA end-to-end length.

Third, to verify that the observed handedness is measured for full octameric nucleosomes rather than tetrasomes, we also examined H3/H4 tetrasomes. In agreement with previous results,[18,19] the obtained H3/H4 tetrasome rotation curves were qualitatively different from those for complete nucleosomes. Instead of having a similar-shaped, but shifted rotation curve, the rotation curves after tetrasome assembly significantly broadened and did not change its center position (Fig. S4C†). As was documented previously, the reason for these broad curves is that in contrast to nucleosomes, tetrasomes can easily switch between a left- and right-handed chirality.[18] Tetrasomes therefore switch into a right-handed conformation when positive torsion is applied, whereas negative torsion pushes all tetrasomes into a left-handed conformation – yielding very broad rotation curves centered at zero. Nucleosomes, by contrast, maintain their handedness even when applying subsequent torque on the DNA. The well-defined shifted rotation curves of Fig. 2 and S2† therefore, cannot be ascribed to tetrasomes. In a separate experiment, a two-step assembly of nucleosomes was performed. In an earlier study[18] we showed that full octameric nucleosomes can be assembled in two separate steps: in step 1 as tetrasomes and only in step 2 as full nucleosomes. Briefly (for details see Fig. S5†), we first assembled H3–H4 histones onto the DNA. Then, we flushed out all unbound NAP1 and histones, followed by flushing in histones H2A and H2B preincubated with NAP1, which led to further assembly into complete nucleosomes. Note that the DNA molecule was rotationally constrained in these assembly experiments. At zero applied turns, H3–H4 tetramers were assembled leading to the expected broadened rotation curve, where the broadening of 6 turns indicated assembly of 3 to 4 tetramers (Fig. S5D†).[18] Next, unbound NAP1 and H3–H4 histones were flushed out, +12 positive rotations were applied, and NAP1 preincubated with histones H2A and H2B were flushed in, leading to (i) further compaction of the DNA, (ii) a nonwidened rotation curve (with a width similar to bare DNA), and (iii) a shift in the rotation curve of +3 ± 1 turns (Fig. S5C and E†). This experiment convincingly showed that a shift of the rotation curve exclusively occurs when full nucleosomes are assembled.

Taken together, the data indicate that the positive chirality of both H3 and CENP-A nucleosomes assembled on positively supercoiled DNA requires assembly of nucleosomes containing all four histones, *i.e.*, H3/CENP-A, H2A, H2B and H4.

Compaction upon nucleosome assembly is similar for negatively and positively supercoiled DNA

When a DNA molecule is wrapped around the histone octamer, the DNA linking number changes due to the chiral wrapping, while at the same time the end-to-end length of the DNA is decreased due to the DNA that is absorbed in the wrap.

Our magnetic-tweezer assay allows independent measurement of the over/under winding of the linker DNA and the DNA compaction due to nucleosome formation. The latter can be deduced from the difference in Z between the maxima of the rotation curves before and after nucleosome assembly. This ΔZ length change allows us to study the compaction upon nucleosome assembly as a function of the total linking number of the assembled nucleosomes ($\Delta L_{k,nuc}$).

The observed relation between the amount of nucleosome-induced compaction and the total shift in the rotation curve (*i.e.* the induced change in nucleosome linking number $\Delta L_{k,nuc}$) is shown in Fig. 3B. For direct comparison between nucleosomes that were assembled on either positively or negatively supercoiled DNA molecules, ΔZ is shown as a function of the absolute value of $\Delta L_{k,nuc}$. We observe that ΔZ scales with $\Delta L_{k,nuc}$, *i.e.*, the larger the nucleosome-induced compaction, the larger the total linking number of the nucleosomes. This is as expected since both ΔZ and $\Delta L_{k,nuc}$ scale linearly with the number of assembled nucleosomes. A linear fit to the data (red line) shows that the compaction amounts to 63 ± 7 nm (slope ± standard deviation) per turn of nucleosomal DNA, in agreement with previous finding of 56 ± 3 nm per turn.[14,30] This value is also consistent with previous reports that showed that the linking number of a nucleosome is about −1.0,[45–47] the amount of DNA wrapped into a nucleosome is 147 bp, *i.e.*, about 50 nm, and the directly adjacent linker DNA coming off the nucleosome adds a further reduction of the end-to-end length of the dsDNA molecule that is measured. The nucleosome-induced compaction on positively supercoiled DNA (closed symbols) is seen to be similar to that on negatively supercoiled DNA (open symbols). Additionally, again, we observed virtually no difference between H3- (blue squares) and CENP-A- (orange circles) containing nucleosomes.

We also assembled H3 and CENP-A nucleosomes on nicked DNA (black crosses Fig. 3B). Such nicked molecules are rotationally unconstrained and any potential buildup of torque due to nucleosome formation is immediately relaxed by the free rotation of the DNA backbone, hence ΔL_k is maintained at 0 (illustrated in Fig. S6†). Because the DNA is rotationally unconstrained, we cannot measure the linking number of the assembled nucleosomes on nicked DNA. However, the amount of compaction of nicked DNA molecules was similar to that for rotationally constrained molecules. Also, we found no evidence in our data that the amount of applied supercoiling influenced the total number of assembled nucleosomes. Thus, although supercoiling has an effect on the handedness of the nucleosomes, it does not have an effect on the level of compaction. In other words, the absence of supercoiling neither hinders nor stimulates nucleosome assembly.

CENP-A and H3 nucleosomes disassemble with similar disruption steps upon high force pulling

The number of nucleosomes can be determined by analyzing the number of disassembly steps as well as the length of unwrapping DNA, when a high stretching force (above 10 pN) is applied. Previous pulling experiments clearly demonstrated that the 147 bp of DNA in the nucleosome disrupts from the core histone octamer in two steps of ~24 nm each.[14–17] Note that the actual length decrease measured in the tweezers upon assembly is larger than the length decrease upon disassembly due to the much higher stretching force during disassembly which minimizes the length reduction due to linker DNA. Because the crystal structure of the CENP-A nucleosome is virtually superimposable with the octameric H3 nucleosomes,[2] a logical prediction is that it would similarly disassemble into two steps.

Fig. 4A shows a typical example of a measurement of the force-induced H3-nucleosome disassembly steps, where the DNA extension is shown as a function of time when a constant pulling force of 13 pN is applied. We analyzed the disruption step size upon high-force pulling on nicked DNA with H3 and CENP-A nucleosomes (Fig. 4B, blue and orange bars respectively), using a commonly used step-finder algorithm.[7] More than ten individual DNA molecules were used to collect 50 disruption steps for each nucleosome type, using a pulling force of 20 pN to ensure complete nucleosome disassembly. Similar to previous reports,[14–17] we found the nucleosomal disrupture steps to amount about 21 ± 7 nm (mean ± standard deviation) and 21 ± 7 nm for H3 and CENP-A nucleosomes, respectively. A few steps were significantly larger than this 21 nm, which can be

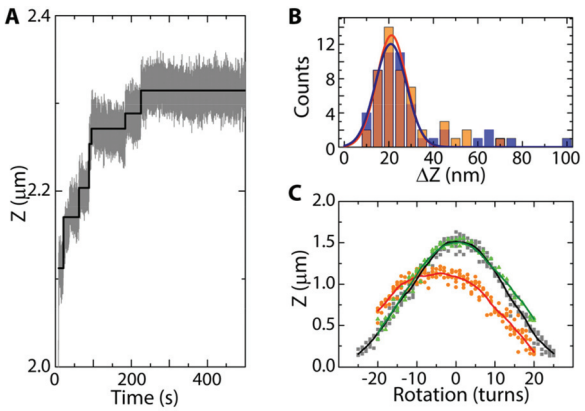

Fig. 4 Nucleosome disassembly upon high-force pulling. (A) DNA end-to-end length Z as a function of time. At t = 10 s the force is abruptly increased from 0.3 pN to 13 pN, after which it is held constant. The DNA extends stepwise due to nucleosome disassembly of H3 nucleosomes. Grey line represents the raw data measured at 100 Hz. Using a step-finding algorithm,[7] the individual disassembly steps are fitted (black line). (B) Histogram of the length increase ΔZ due to force-induced H3 (blue bars) and CENP-A (orange bars) nucleosome disassembly (for steps from at least 10 different nicked DNA molecules each nucleosome type). The step sizes are a signature of nucleosome disassembly.[14–17] Gaussian fits to both histograms yield a peak at 21 ± 7 nm (mean ± standard deviation). (C) Rotation curve before assembly (grey squares), after assembly of CENP-A nucleosomes at negatively supercoiled DNA (orange circles) and after high-force pulling (green triangles). The shift of the rotation curve is a direct measure of the linking number of the assembled nucleosomes, as shown by the fact that the exact same bare DNA curve is recovered after high-force disassembly, in combination with the stepwise disassembly as shown in (A), and comparable to previous nucleosome-disassembly experiments reported in literature.[14–17]

ascribed to multiple simultaneous disruption events that occur at the beginning of the traces where the time separation between individual events is very short. The similar observed disruption step sizes for both H3 and CENP-A nucleosomes suggest a similar disassembly mechanism for both nucleosomes.

By applying high-force pulling, all nucleosomes can be disrupted and the initial bare dsDNA can be obtained again. Fig. 4C shows the initial rotation curve of a bare DNA molecule (grey squares). After the assembly of nucleosomes in the presence of negative supercoiling, the rotation curve (orange circles) shows the compacted molecule with left-handed nucleosomes. After subsequent high-force pulling, the rotation curve (green triangles) is, gratifyingly, again the same as the bare DNA rotation curve measured before the assembly of nucleosomes.

Discussion

In this report, we used magnetic tweezers to address the handedness of nucleosomes that are assembled on DNA. Our data demonstrate that, surprisingly, both canonical H3 nucleosomes as well as CENP-A nucleosomes can assemble with a right-handed chirality on positively supercoiled DNA, whereas they do so, as expected, with a left-handed chirality on negatively supercoiled DNA. We note that these results cannot be attributed to potential tetrasomes (that is, CENP-A_2/$H4_2$ or $H3_2$/$H4_2$ tetramers), as tetrasomes have been excluded with our control experiments and furthermore have been shown to be rotationally flexible and therefore they do not shift the center of the rotation curves.[14,18,19] The dependence of nucleosome handedness on the supercoiling state of DNA revealed in these experiments provides a potential explanation for contradictory data in literature on the existence of left- and right-handed canonical and CENP-A nucleosomes: both can indeed exist. Furthermore, we find that octameric canonical and CENP-A nucleosomes exhibit very similar properties; they have for example the same linking number, the same compaction per nucleosome (63 ± 7 nm per turn), and they likewise disassemble in a two-step process. One interesting implication of these data is that it seems unlikely that CENP-A octameric nucleosomes alone would encode unique structural properties associated with centromeric chromatin *in vivo*.

In vitro, the structure of the CENP-A octameric nucleosome is almost superimposable with that of H3 but has weakened exit/entry DNA contacts due to the lack of a single Arginine in CENP-A's alpha-N helix which is present in H3's N-terminal section.[2,59] This concurrence in crystallographic and AFM data is in contrast with the previously reported rigidified CENP-A/H4 tetrameric core, which is more compact and has been interpreted to be inflexible.[60,61] A potential explanation for the contrast might arise from recent computational modeling experiments which suggest that CENP-A nucleosomes may be adaptable and can shear at the four helix bundles holding together the two pseudo-symmetric halves of the nucleosome.[62] This interpretation is supported, in part, by recent sm-FRET data demonstrating that CENP-A nucleosomal DNA is intrinsically flexible in vitro,[63,64] and that such flexibility is restrained in the presence of kinetochore proteins.

For the left-handed canonical nucleosome, extensive studies have shown that the DNA wraps in 1.7 turns a total of 147 bp of DNA with a total linking number of approximately −1.0.[45–47] Using the known crystal structures, the left-handed canonical and CENP-A nucleosomes have, respectively, 147 bp (50 nm) and a minimum amount of 122 bp (41 nm) DNA wrapped around the histone core.[1,2] We note that our measured value of $\Delta Z/|\Delta L_{k,nuc}|$ of −63 ± 7 nm per turn from the data of Fig. 3B likely represent an upper bound due to the decrease in driving supercoiling with increasing numbers of assembled nucleosomes (as discussed previously and illustrated in Fig. S3C and D†). Fitting ΔZ/abs ($\Delta L_{k,nuc}$) for one third of the data with the smallest compaction per $|\Delta L_{k,nuc}|$ indeed gives a linking number of ±1.0 per 56 nm of compaction (Fig. S7†), in good agreement with the vast amount of literature on left-handed canonical nucleosomes.

The most surprising – and profound – aspect of our study is that nucleosomes are readily formed with presumably right-handed chirality if the DNA substrate is already positively supercoiled. The presence of right-handed nucleosomes might present a mechanism through which positive torsional stress can be removed from the DNA. Potentially such nucleosomes may provide a topological "memory" of local positive supercoiling, until such stretches are remodeled, transcribed, replicated or perhaps flip handedness under the influence of an increased build-up of torsion.[8,28] We cautiously note that we cannot, from these experiments, conclude how exactly nucleosomes tolerate positively supercoiled DNA. In addition to the simplest possibility, that of right-handed octamers, alternative explanations include induction of hitherto unknown internal conformational changes in H3 and CENP-A nucleosomes such as internal bubbling of a pseudo-dyad proximal DNA loop, or altered gyration of the entry/exit DNA.

Regardless of the mechanism by which positive supercoiling is accommodated, we find that the H3 and CENP-A octameric nucleosomes generally exhibit nearly identical wrapping and compaction, both on negatively and positively supercoiled DNA templates. Previously, it was suggested that a different handedness of the centromeric CENP-A nucleosome could serve as a key distinguishing structural mark of the active centromere.[9] Recently Díaz-Ingelmo[10] showed that a positively supercoiled loop of ~70 bp centromeric DNA was essential to form a centromere nucleosome with a linking number of +0.6, indicative of a right-handed CENP-A species as already described in very early work.[9,65] Our data provide support for this result. However, our experiments suggest that the sole replacement of H3 by CENP-A does not induce a change in the nucleosome structure from left- to right-handed. Instead, our results show that nucleosome handedness is controlled by the state of DNA supercoiling. *In vivo*, this may result from the action of chromatin remodelers, chaperones or other topological modifiers (*e.g.* transcription or replication), or sequence-

dependent DNA structures, which may create a template that preferentially generates one type of nucleosome handedness over the other.

Our study shows that both left- and right-handed nucleosomes can be formed, dependent on the supercoiling state of the DNA upon which they assemble. Our data thus support recent advances suggesting a surprising intrinsic adaptability of the nucleosomal structure, and provide insights into how nucleosomes might rapidly re-assemble after mechanical processes that generate positive supercoiling *in vivo*.

Author contributions

RV, SHK, PdZ, YD and CD planned the experiments; RV, SHK and PdZ performed the experiments; RV, SHK, PdZ, YD and CD analyzed and discussed the data; RV, YD and CD wrote the manuscript.

Funding

This work was supported by the ERC Advanced Grant SynDiv [grant number 669598 to C. D.]; the Netherlands Organization for Scientific Research (NWO/OCW) [part of the Frontiers of Nanoscience program, to C. D.]; and by the Intramural Research Program of the Center for Cancer Research, NCI, NIH, USA [Y. D.].

Acknowledgements

We thank Alexandra Lusser for the kind gift of recombinant NAP1 and core histones and Catherine Volle, Marc Bailly and Marcin Walkiewicz (Dalal lab) for recombinant CENP-A, H3, H2A, H2B and H4. We thank members of the Dekker and Dalal labs for discussions and comments on the manuscript. YD thanks David Clark (NIH) and Minou Bina (Purdue) for thoughtful discussions on chromatin assembly on positively supercoiled templates.

References

1 K. Luger, A. W. Mader, R. K. Richmond, D. F. Sargent and T. J. Richmond, *Nature*, 1997, **389**, 251–260.
2 H. Tachiwana, W. Kagawa, T. Shiga, A. Osakabe, Y. Miya, K. Saito, Y. Hayashi-Takanaka, T. Oda, M. Sato, S. Y. Park, H. Kimura and H. Kurumizaka, *Nature*, 2011, **476**, 232–235.
3 A. L. Olins and D. E. Olins, *Science*, 1974, **183**, 330–332.
4 R. D. Kornberg, *Annu. Rev. Biochem.*, 1977, **46**, 931–954.
5 B. Brower-Toland, D. A. Wacker, R. M. Fulbright, J. T. Lis, W. L. Kraus and M. D. Wang, *J. Mol. Biol.*, 2005, **346**, 135–146.
6 T. J. Richmond and C. A. Davey, *Nature*, 2003, **423**, 145–150.
7 J. W. Kerssemakers, E. L. Munteanu, L. Laan, T. L. Noetzel, M. E. Janson and M. Dogterom, *Nature*, 2006, **442**, 709–712.
8 A. Bancaud, G. Wagner, E. S. N. Conde, C. Lavelle, H. Wong, J. Mozziconacci, M. Barbi, A. Sivolob, E. Le Cam, L. Mouawad, J. L. Viovy, J. M. Victor and A. Prunell, *Mol. Cell*, 2007, **27**, 135–147.
9 T. Furuyama and S. Henikoff, *Cell*, 2009, **138**, 104–113.
10 O. Díaz-Ingelmo, B. Martínez-García, J. Segura, A. Valdés and J. Roca, *Cell Rep.*, 2015, **13**, 667–677.
11 S. L. Pereira and J. N. Reeve, *Extremophiles*, 1998, **2**, 141–148.
12 S. L. Pereira, R. A. Grayling, R. Lurz and J. N. Reeve, *Proc. Natl. Acad. Sci. U. S. A.*, 1997, **94**, 12633–12637.
13 P. B. Talbert and S. Henikoff, *Nat. Rev. Mol. Cell Biol.*, 2010, **11**, 264–275.
14 R. Vlijm, J. S. Smitshuijzen, A. Lusser and C. Dekker, *PLoS One*, 2012, **7**, e46306.
15 B. D. Brower-Toland, C. L. Smith, R. C. Yeh, J. T. Lis, C. L. Peterson and M. D. Wang, *Proc. Natl. Acad. Sci. U. S. A.*, 2002, **99**, 1960–1965.
16 F. T. Chien and J. van Noort, *Curr. Pharm. Biotechnol.*, 2009, **10**, 474–485.
17 C. Claudet, D. Angelov, P. Bouvet, S. Dimitrov and J. Bednar, *J. Biol. Chem.*, 2005, **280**, 19958–19965.
18 R. Vlijm, M. Lee, J. Lipfert, A. Lusser, C. Dekker and N. H. Dekker, *Cell Rep.*, 2015, **10**, 216–225.
19 R. Vlijm, M. Lee, O. Ordu, A. Boltengagen, A. Lusser, N. H. Dekker and C. Dekker, *PLoS One*, 2015, **10**, e0141267.
20 A. J. Katan, R. Vlijm, A. Lusser and C. Dekker, *Small*, 2015, **11**, 976–984.
21 A. Hamiche, V. Carot, M. Alilat, F. De Lucia, M. F. O'Donohue, B. Revet and A. Prunell, *Proc. Natl. Acad. Sci. U. S. A.*, 1996, **93**, 7588–7593.
22 A. Hamiche and H. Richard-Foy, *J. Biol. Chem.*, 1998, **273**, 9261–9269.
23 M. Alilat, A. Sivolob, B. Révet and A. Prunell, *J. Mol. Biol.*, 1999, **291**, 815–841.
24 D. J. Clark and G. Felsenfeld, *EMBO J.*, 1991, **10**, 387–395.
25 P. Pfaffle and V. Jackson, *J. Biol. Chem.*, 1990, **265**, 16821–16829.
26 C. Lavelle, P. Recouvreux, H. Wong, A. Bancaud, J. L. Viovy, A. Prunell and J. M. Victor, *Cell*, 2009, **139**, 1216–1217; author reply 1217–1218.
27 G. Wieland, S. Orthaus, S. Ohndorf, S. Diekmann and P. Hemmerich, *Mol. Cell. Biol.*, 2004, **24**, 6620–6630.
28 F. Kouzine, A. Gupta, L. Baranello, D. Wojtowicz, K. Ben-Aissa, J. Liu, T. M. Przytycka and D. Levens, *Nat. Struct. Mol. Biol.*, 2013, **20**, 396–403.
29 C. Naughton, N. Avlonitis, S. Corless, J. G. Prendergast, I. K. Mati, P. P. Eijk, S. L. Cockroft, M. Bradley, B. Ylstra and N. Gilbert, *Nat. Struct. Mol. Biol.*, 2013, **20**, 387–395.
30 A. Bancaud, N. Conde e Silva, M. Barbi, G. Wagner, J. F. Allemand, J. Mozziconacci, C. Lavelle, V. Croquette, J. M. Victor, A. Prunell and J. L. Viovy, *Nat. Struct. Mol. Biol.*, 2006, **13**, 444–450.
31 M. Gellert, K. Mizuuchi, M. H. O'Dea and H. A. Nash, *Proc. Natl. Acad. Sci. U. S. A.*, 1976, **73**, 3872–3876.
32 D. J. Clark and A. P. Wolffe, *EMBO J.*, 1991, **10**, 3419–3428.
33 G. Snounou and A. D. Malcom, *J. Mol. Biol.*, 1983, **167**, 211–216.

34 C. Gosse and V. Croquette, *Biophys. J.*, 2002, **82**, 3314–3329.
35 K. Luger, T. J. Rechsteiner and T. J. Richmond, *Methods Mol. Biol.*, 1999, **119**, 1–16.
36 M. P. Walkiewicz, M. Bui, D. Quenet and Y. Dalal, *Methods Mol. Biol.*, 2014, **1170**, 589–615.
37 A. J. Andrews, X. Chen, A. Zevin, L. A. Stargell and K. Luger, *Mol. Cell*, 2010, **37**, 834–842.
38 J. Mazurkiewicz, J. F. Kepert and K. Rippe, *J. Biol. Chem.*, 2006, **281**, 16462–16472.
39 T. Nakagawa, M. Bulger, M. Muramatsu and T. Ito, *J. Biol. Chem.*, 2001, **276**, 27384–27391.
40 T. Fujii-Nakata, Y. Ishimi, A. Okuda and A. Kikuchi, *J. Biol. Chem.*, 1992, **267**, 20980–20986.
41 S. H. Kim, R. Vlijm, J. van der Torre, Y. Dalal and C. Dekker, *PLoS One*, 2016, **11**, e0165078.
42 G. Arents, R. W. Burlingame, B. C. Wang, W. E. Love and E. N. Moudrianakis, *Proc. Natl. Acad. Sci. U. S. A.*, 1991, **88**, 10148–10152.
43 J. Widom, *Annu. Rev. Biophys. Biophys. Chem.*, 1989, **18**, 365–395.
44 T. J. Richmond, J. T. Finch, B. Rushton, D. Rhodes and A. Klug, *Nature*, 1984, **311**, 532–537.
45 J. E. Germond, B. Hirt, P. Oudet, M. Gross-Bellark and P. Chambon, *Proc. Natl. Acad. Sci. U. S. A.*, 1975, **72**, 1843–1847.
46 R. T. Simpson, F. Thoma and J. M. Brubaker, *Cell*, 1985, **42**, 799–808.
47 V. G. Norton, B. S. Imai, P. Yau and E. M. Bradbury, *Cell*, 1989, **57**, 449–457.
48 J. Lipfert, S. Klijnhout and N. H. Dekker, *Nucleic Acids Res.*, 2010, **38**, 7122–7132.
49 D. J. Clark, R. Ghirlando, G. Felsenfeld and H. Eisenberg, *J. Mol. Biol.*, 1993, **234**, 297–301.
50 D. R. Hewish and L. A. Burgoyne, *Biochem. Biophys. Res. Commun.*, 1973, **52**, 504–510.
51 A. Stein, Y. Dalal and T. J. Fleury, *Nucleic Acids Res.*, 2002, **30**, 5103–5109.
52 C. Bouchiat, M. D. Wang, J. Allemand, T. Strick, S. M. Block and V. Croquette, *Biophys. J.*, 1999, **76**, 409–413.
53 T. Strick, J.-F. Allemand, V. Croquette and D. Bensimon, *Prog. Biophys. Mol. Biol.*, 2000, **74**, 115–140.
54 J. van Noort, S. Verbrugge, N. Goosen, C. Dekker and R. T. Dame, *Proc. Natl. Acad. Sci. U. S. A.*, 2004, **101**, 6969–6974.
55 I. D. Vladescu, M. J. McCauley, I. Rouzina and M. C. Williams, *Phys. Rev. Lett.*, 2005, **95**, 158102.
56 M. McCauley, P. R. Hardwidge, L. J. Maher 3rd and M. C. Williams, *Biophys. J.*, 2005, **89**, 353–364.
57 M. L. Bennink, O. D. Schärer, R. Kanaar, K. Sakata-Sogawa, J. M. Schins, J. S. Kanger, B. G. de Grooth and J. Greve, *Cytometry*, 1999, **36**, 200–208.
58 M. Lee, J. Lipfert, H. Sanchez, C. Wyman and N. H. Dekker, *Nucleic Acids Res.*, 2013, **41**, 7023–7030.
59 M. P. Walkiewicz, E. K. Dimitriadis and Y. Dalal, *Nat. Struct. Mol. Biol.*, 2014, **21**, 2–3.
60 N. Sekulic, E. A. Bassett, D. J. Rogers and B. E. Black, *Nature*, 2010, **467**, 347–351.
61 M. D. Miell, C. J. Fuller, A. Guse, H. M. Barysz, A. Downes, T. Owen-Hughes, J. Rappsilber, A. F. Straight and R. C. Allshire, *Nat. Struct. Mol. Biol.*, 2013, **20**, 763–765.
62 D. Winogradoff, H. Zhao, Y. Dalal and G. A. Papoian, *Sci. Rep.*, 2015, **5**, 17038.
63 S. J. Falk, L. Y. Guo, N. Sekulic, E. M. Smoak, T. Mani, G. A. Logsdon, K. Gupta, L. E. Jansen, G. D. Van Duyne, S. A. Vinogradov, M. A. Lampson and B. E. Black, *Science*, 2015, **348**, 699–703.
64 S. J. Falk, J. Lee, N. Sekulic, M. A. Sennett, T. H. Lee and B. E. Black, *Nat. Struct. Mol. Biol.*, 2016, **23**, 204–208.
65 K. S. Bloom, E. Amaya, J. Carbon, L. Clarke, A. Hill and E. Yeh, *J. Cell Biol.*, 1984, **99**, 1559–1568.

